NASA TM X-239

NASA

TECHNICAL MEMORANDUM
X-239

FIN LOADS AND TIP-CONTROL HINGE MOMENTS ON A 1/8-SCALE MODEL

SIMULATING THE FIRST STAGE OF THE SCOUT RESEARCH

VEHICLE AT A MACH NUMBER OF 2.01

By Ross B. Robinson and Emma Jean Landrum

Langley Research Center
Langley Field, Va.

NATIONAL AERONAUTICS AND SPACE ADMINISTRATION

WASHINGTON   April 1960

OTS PRICE

$
ILM $

CONFIDENTIAL

DI-60-4-26-74

NATIONAL AERONAUTICS AND SPACE ADMINISTRATION

TECHNICAL MEMORANDUM X-239

FIN LOADS AND TIP-CONTROL HINGE MOMENTS ON A 1/8-SCALE MODEL

SIMULATING THE FIRST STAGE OF THE SCOUT RESEARCH

VEHICLE AT A MACH NUMBER OF 2.01*

By Ross B. Robinson and Emma Jean Landrum

SUMMARY

17464

An investigation has been conducted at a Mach number of 2.01 in the Langley 4- by 4-foot supersonic pressure tunnel to determine the fin loads and tip-control hinge moments on a 1/8-scale model simulating the first stage of the Scout research vehicle. The model was a body of revolution with cruciform, 45° delta tail fins.

For the range of this investigation, hinge moment was small and varied nonlinearly with control deflection. Roll angle had no effect on the control-effectiveness parameters which were relatively constant throughout the angle-of-attack range.

INTRODUCTION

An investigation has been made to determine the fin loads and tip-control hinge moments for a 1/8-scale model simulating the first stage of the Scout research vehicle at a Mach number of 2.01 in the Langley 4- by 4-foot supersonic pressure tunnel. The model was composed of a body of revolution with cruciform, 45° delta tail fins. One of the fins was instrumented for measuring panel loads and was equipped with a movable tip control attached to a hinge-moment beam inside the fin. The tests were made to obtain data needed in the design of the tip-control actuator mechanism and to provide loads information on which the fin structural design could be based.

This report presents fin loads and tip-control hinge-moment data for various control deflections for an angle-of-attack range from -6° to 6° at zero sideslip for roll angles of 0°, 45°, and 90°. The data are presented without analysis.

_____
*Title, Unclassified.

2

SYMBOLS

The results are referred to the body-axis system, with all the moment coefficients except the rolling-moment and hinge-moment coefficients referred to the 67-percent-chord station of the fin root chord. The rolling-moment coefficient is referred to the model center line and the hinge-moment coefficient to the hinge line of the tip control. A sketch of the axis system is presented in figure 1.

b	fin span, exposed single panel
C_A	axial-force coefficient, F_A/qS
C_b	root-bending-moment coefficient, M_b/qSb
C_h	control hinge-moment coefficient, $M_h/qS_t\bar{c}_t$
C_l	rolling-moment coefficient, M_X/qSb
C_m	pitching-moment coefficient, $M_Y/qS\bar{c}$
C_N	normal-force coefficient, F_N/qS
C_s	shearing-moment coefficient, $M_s/qS\bar{c}$
C_Y	side-force coefficient, F_Y/qS
$\bar{c}$	fin mean geometric chord
$\bar{c}_t$	tip-control mean geometric chord
F_A	fin axial force
F_N	fin normal force
F_Y	side force
M_b	root-bending moment, moment about fin root chord
M_h	hinge moment, hinge line at 63 percent of control root chord
M_s	shearing moment, moment about Z-axis

M_X rolling moment, moment about model center line

M_Y pitching moment, moment about Y-axis

q   free-stream dynamic pressure

S   fin area, exposed

S_t tip-control area

α angle of attack of model center line, deg

δ_t tip-control deflection, positive when trailing edge is to right, deg (fig. 1)

ϕ roll angle, deg

Subscripts:

α rate of change of quantity with respect to angle of attack

δ rate of change of quantity with respect to control deflection

MODEL AND APPARATUS

Details of the model are shown in figure 2, and a photograph is presented in figure 3. The geometric characteristics of the model are as follows:

Body:
  Length, in. 39.50
  Diameter, in. 4.94

Fin (exposed):
  Area (includes control), sq in. 14.79
  Span, in. 5.44
  Root chord, in. 5.44
  Mean geometric chord, in. 3.63
  Leading-edge sweep, deg 45
  Airfoil section, normal to leading edge . . . . 11.3° wedge

Control:
Area, sq in. 0.70
Span, in. 1.18
Root chord, in. 1.18
Mean geometric chord, in. 0.79
Hinge-line location, in. ahead of trailing edge 0.44
Leading-edge sweep, deg 45
Airfoil section, normal to leading edge . . . . 11.3° wedge

The model was composed of a body of revolution with cruciform, 45° delta tail fins having rounded leading edges and blunt trailing edges (fig. 2). Three of the fins were mounted to the body; the fourth fin was attached by a strut to a six-component strain-gage balance located inside the model. The base of the instrumented fin and its strut were separated from the body by 0.03-inch gaps. The instrumented fin was equipped with a manually adjustable tip control attached to a hinge-moment beam mounted inside the fin. The hinge line of the tip control was at the 63-percent-chord station of the control root chord. Transition was fixed on both top and bottom surfaces of the fin and control by means of a 1/8-inch-wide strip of No. 60 carborundum grains along the 10-percent-local-chord line.

The fin geometry and the ratio of the fin span to body diameter simulated the first stage of a 1/8-scale model of the Scout research vehicle; a pointed nose was substituted for the second, third, and fourth stages. Subsequent to this investigation, configuration changes in the Scout research vehicle resulted in a slight reduction in fin area with no change in tip-control dimensions and a rearward movement of the control hinge line to the 67-percent-chord station of the control root chord.

The model was mounted in the tunnel on a manually adjustable sting.

TEST, CORRECTIONS, AND ACCURACY

The test conditions were as follows:

Mach number 2.01
Stagnation temperature, °F 110
Stagnation pressure, lb/sq in. abs 10
Reynolds number per foot . . . . 2.41×10^6

The stagnation dewpoint was maintained sufficiently low (-25° F or less) to avoid condensation effects in the test section.

CONFIDENTIAL

5

Tests were made through an angle-of-attack range from approximately -6° to 6° at roll angles of 0°, 45°, and 90°.

The angles of attack and roll were not corrected for the deflection of the balance and sting under load. No corrections for base pressure have been applied to the results. No forces and moments were measured for the body and attached fins.

The estimated accuracy of the Mach number is ±0.015, and that of the individual measured quantities is as follows:

C_A . . . . ±0.001

C_b . . . . ±0.002

C_h . . . . ±0.006

C_l . . . . ±0.001

C_m . . . . ±0.003

C_N . . . . ±0.002

C_s . . . . ±0.002

C_Y . . . . ±0.005

α, deg . . . . ±0.1

δ_t, deg . . . . ±0.1

ϕ, deg . . . . ±0.1

SUMMARY OF RESULTS

The results of this investigation are presented as follows:

Figure

Schlieren photographs of the flow past the first stage of a
   simulated Scout research vehicle at control deflections of
   0° and -20° for roll angles of 45° and 90°   4
Effect of control deflection on normal-force, axial-force,
   and pitching-moment coefficients for various roll angles   5
Effect of control deflection on side-force and shearing-
   moment coefficients for various roll angles   6
Effect of control deflection on root-bending-moment and
   rolling-moment coefficients for various roll angles   7
Effect of control deflection on the hinge-moment coefficients
   for roll angles of 0° and 90°.   8

No analysis of the results of this investigation is presented; however, it is of interest to note that all the coefficients varied linearly

with α and δ_t at $\phi = 0^\circ$ with the exception of C_h which varied nonlinearly with δ_t. At $\alpha = 0^\circ$, control deflection had no effect on the slope with respect to angle of attack of the curves of the normal-force, root-bending-moment, and hinge-moment coefficients. The slopes of these curves at $\alpha = 0^\circ$ and $\delta_t = 0^\circ$ for the various roll angles are as follows:

ϕ, deg	C_{b_α}	C_{h_α}	C_{N_α}
0	0	0	0
45	.0155	-----	.043
90	.0217	-.007	.060

The values of the control-effectiveness parameters between $\delta_t = 0^\circ$ and $\delta_t = -10^\circ$ at $\phi = 0^\circ$ are

$$C_{b_\delta} = 0.0015$$

$$C_{h_\delta} = -0.0027$$

$$C_{l_\delta} = -0.0027$$

$$C_{m_\delta} = -0.0021$$

$$C_{N_\delta} = 0.0021$$

There is no change in these parameters with either angle of attack or roll angle.

Langley Research Center,
 National Aeronautics and Space Administration,
 Langley Field, Va., November 9, 1959.

CONFIDENTIAL

7
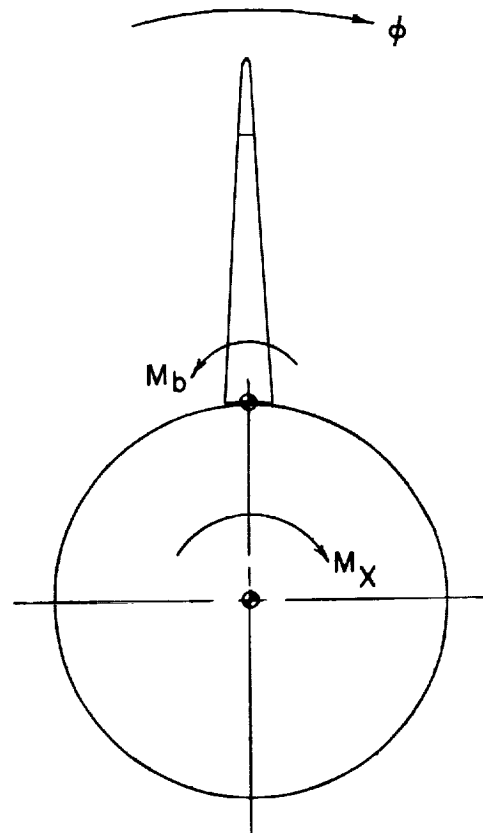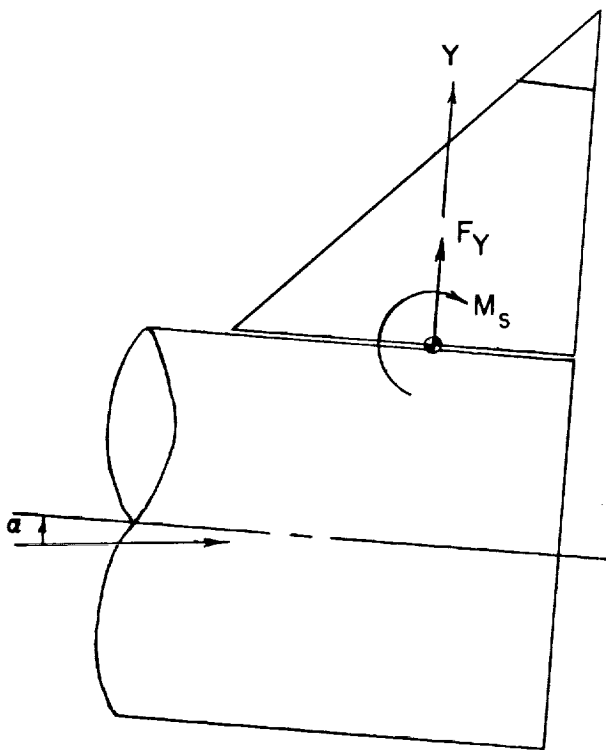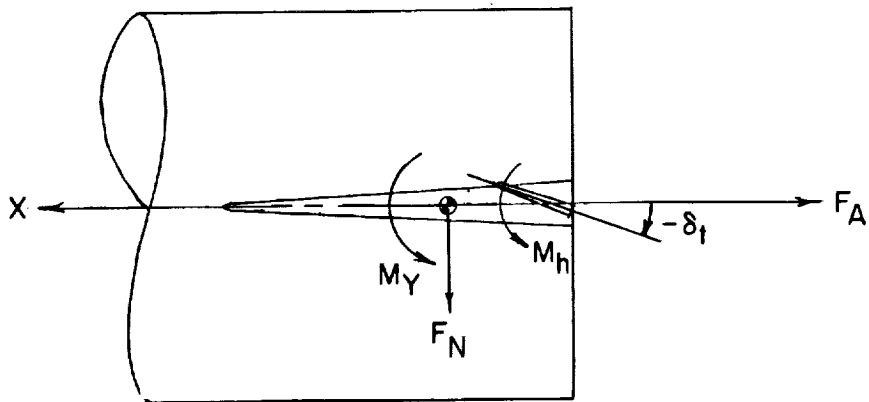
Figure 1.- Axis system. Arrows indicate positive directions except as noted. Model is shown at $\phi = 0^O$.
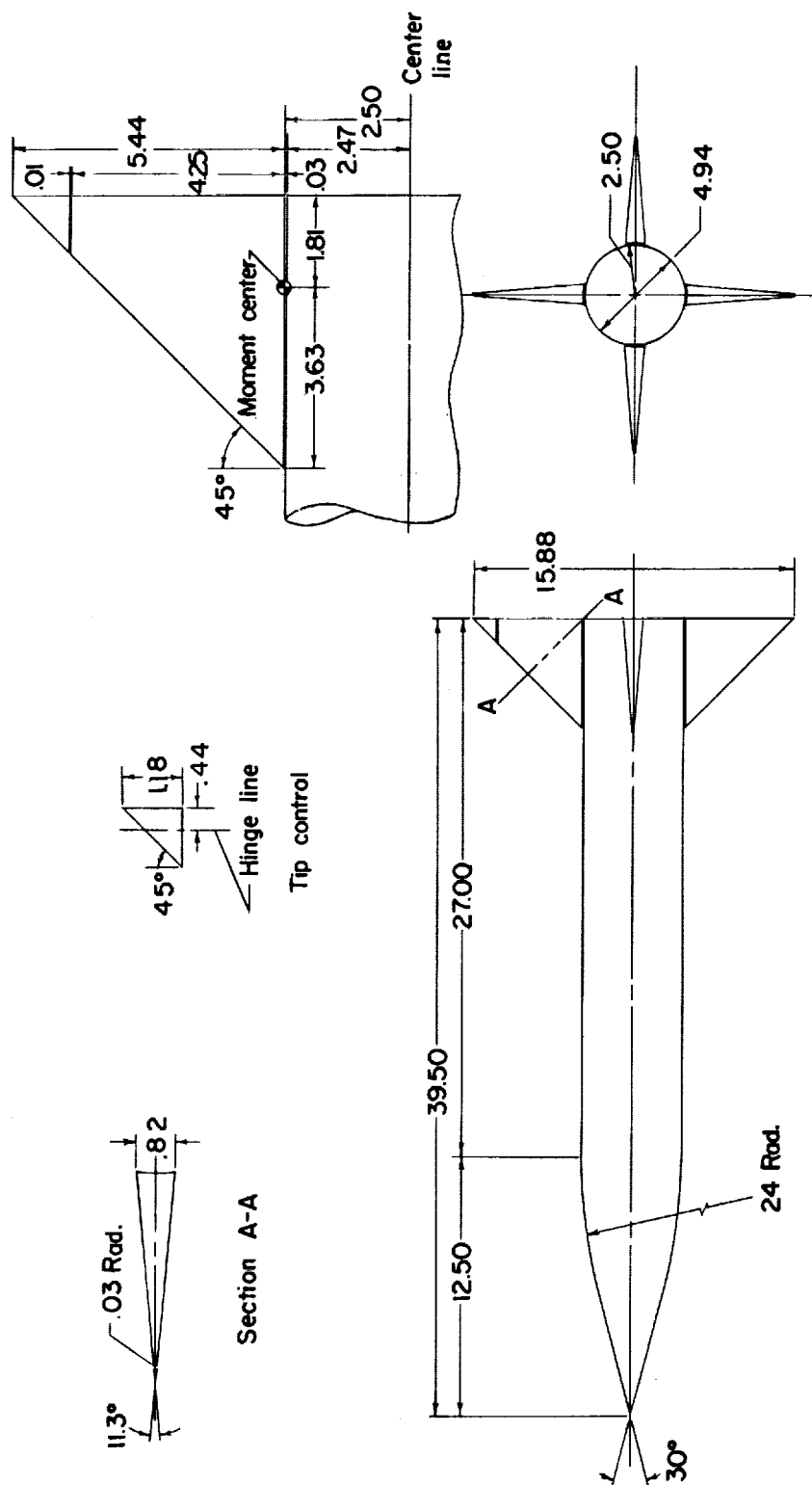
Figure 2.- Details of model. All linear dimensions are in inches.
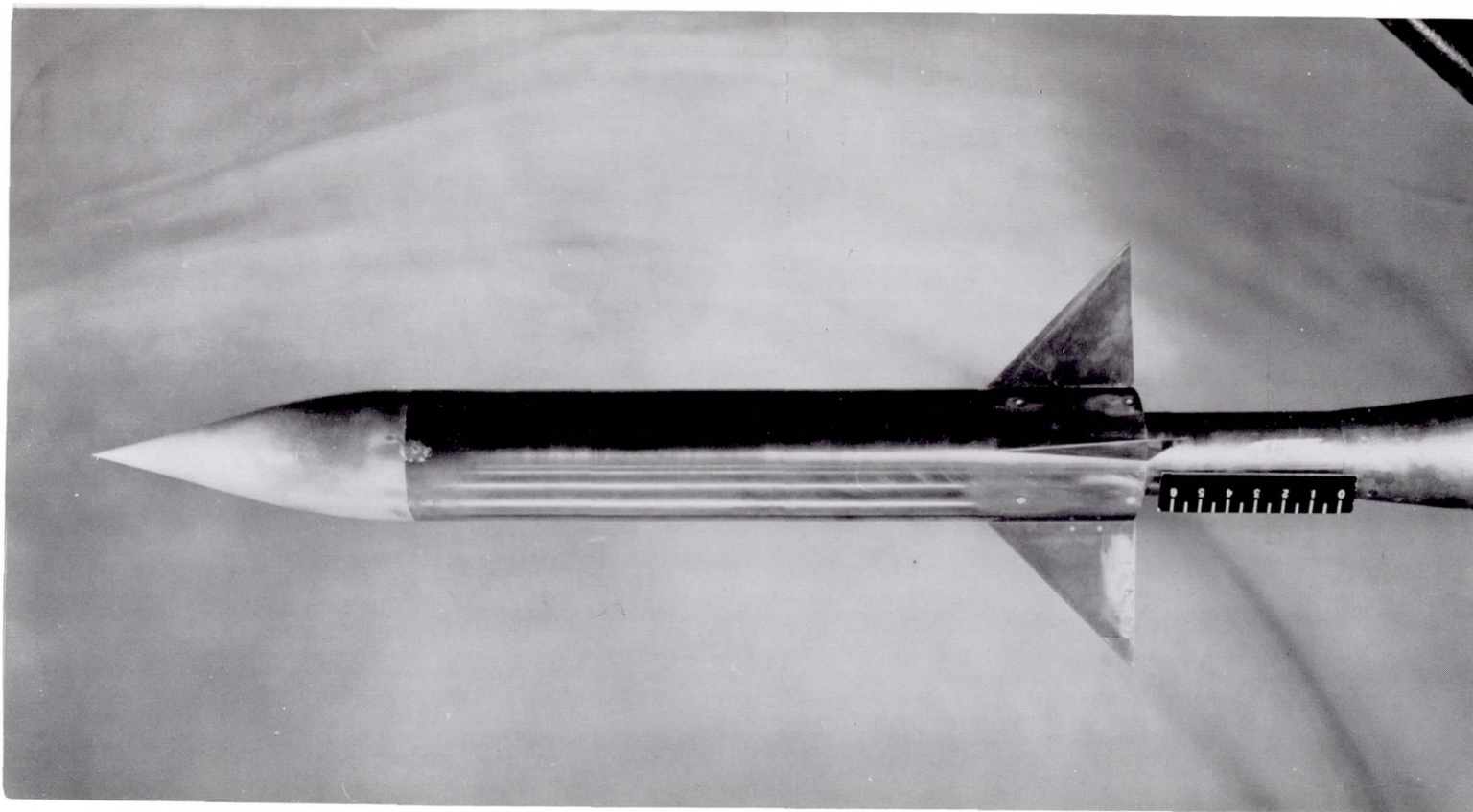
L-59-3514

Figure 3.- Photograph of the simulated 1/8-scale model of the first stage of the Scout research vehicle.
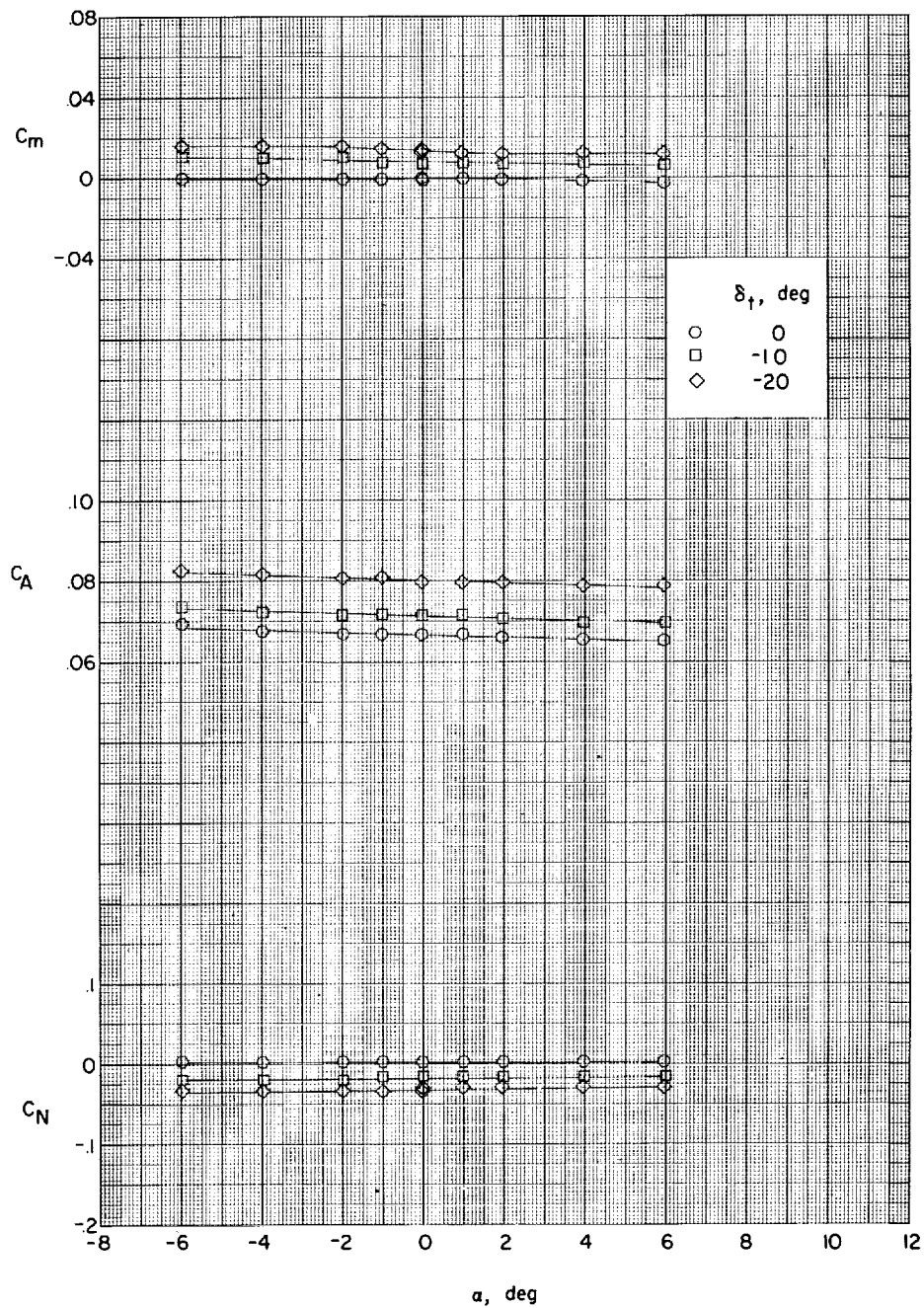
$\phi = 45°$

$\phi = 90°$
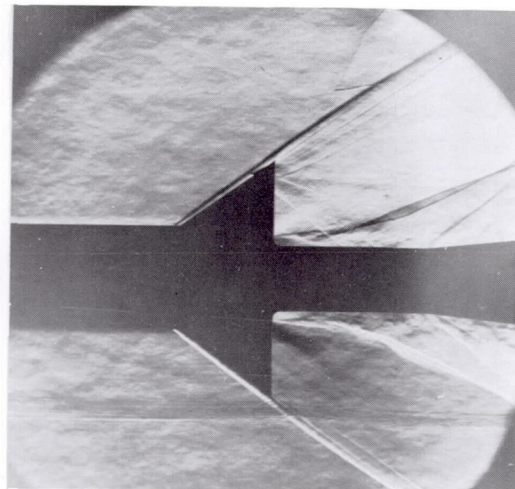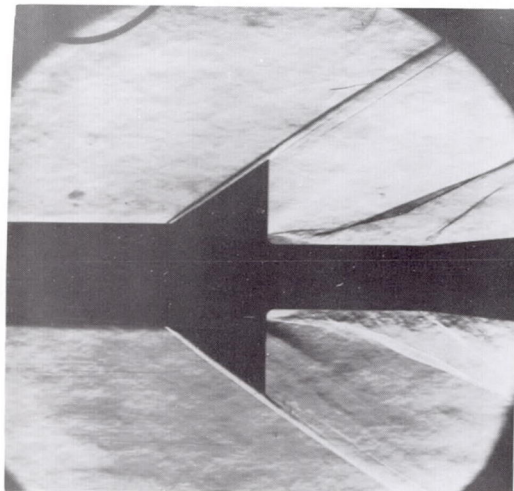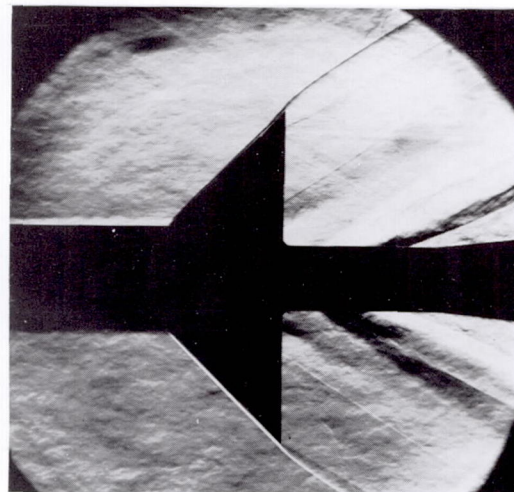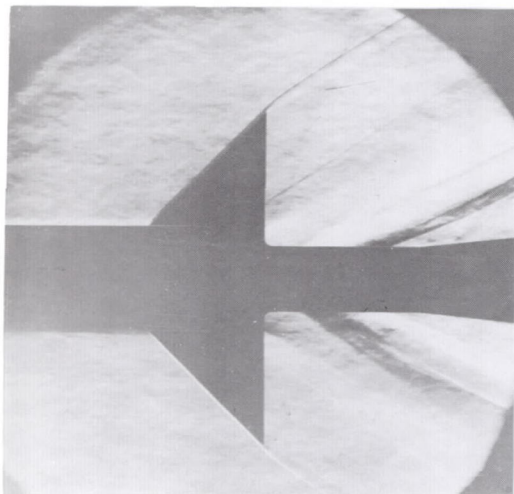
$\delta_t = 0°$ $\delta_t = -20°$

L-59-6490

Figure 4.- Schlieren photographs of the flow past the first stage of a
simulated Scout research vehicle at control deflections of 0° and
-20° for roll angles of 45° and 90°.

11

(a) $\phi = 0°$.

Figure 5.- Effect of control deflection on normal-force, axial-force, and pitching-moment coefficients for various roll angles.
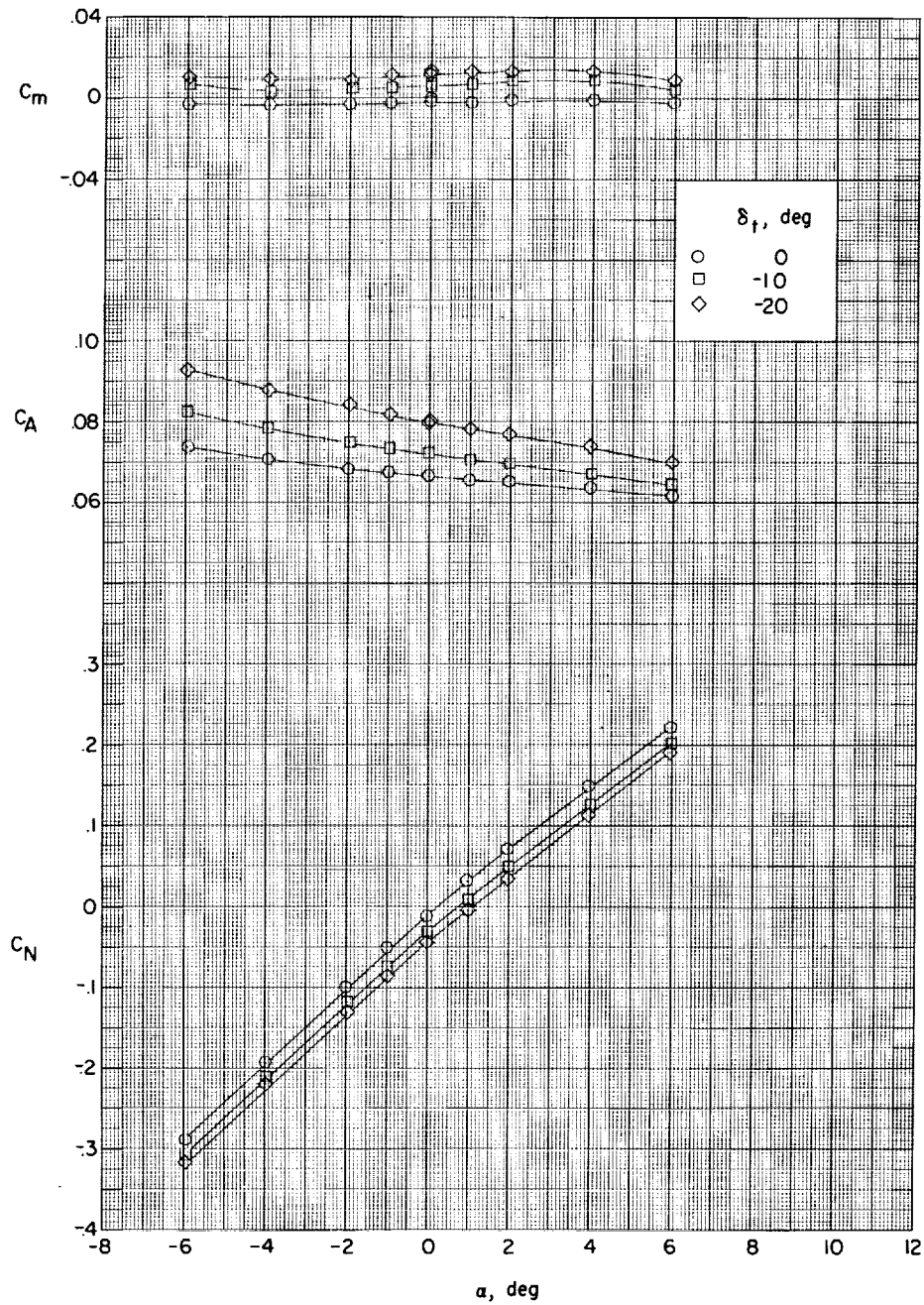
(b) $\phi = 45°$.

Figure 5.- Continued.
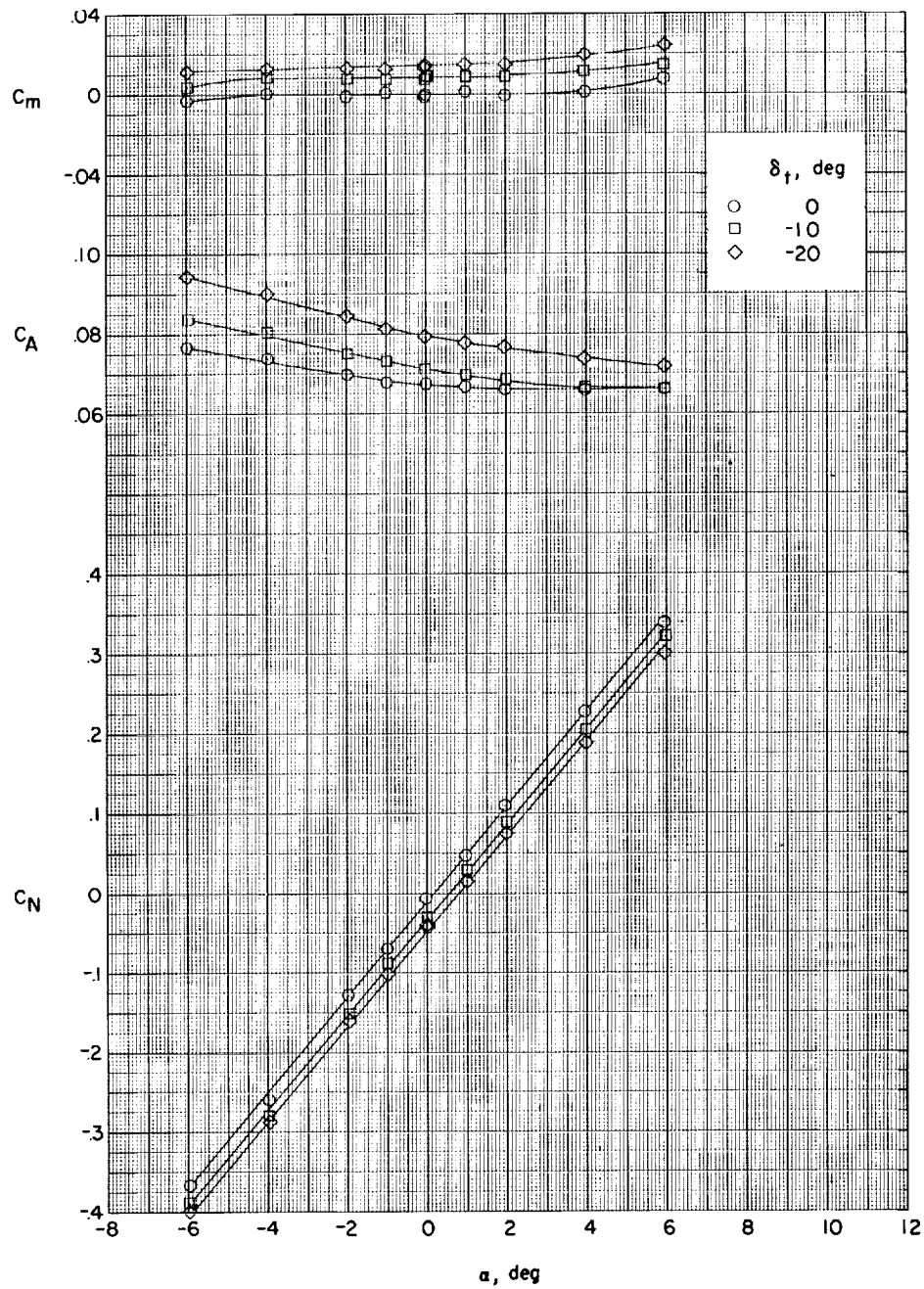
(c) $\phi = 90°$.
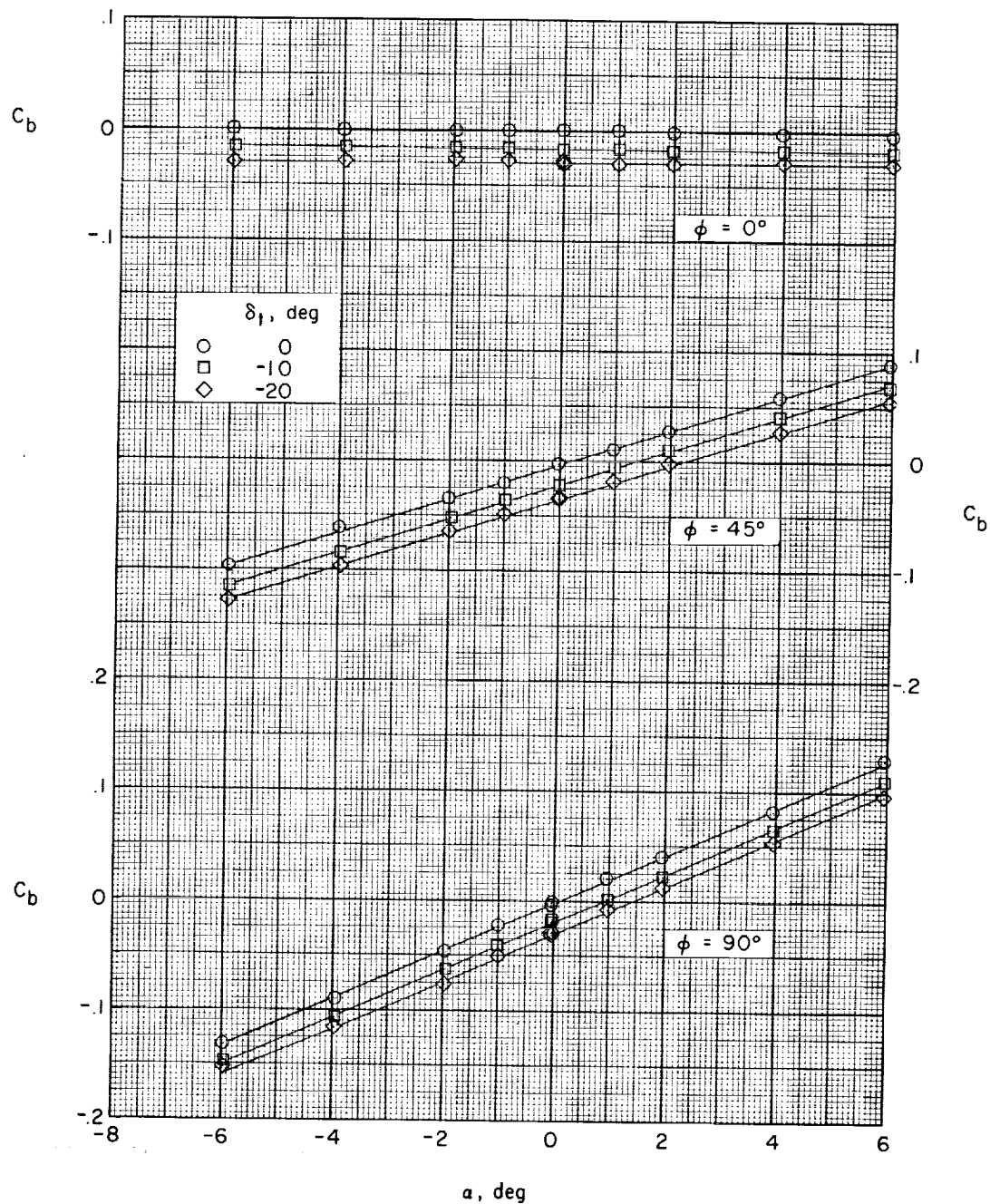
Figure 5.- Concluded.
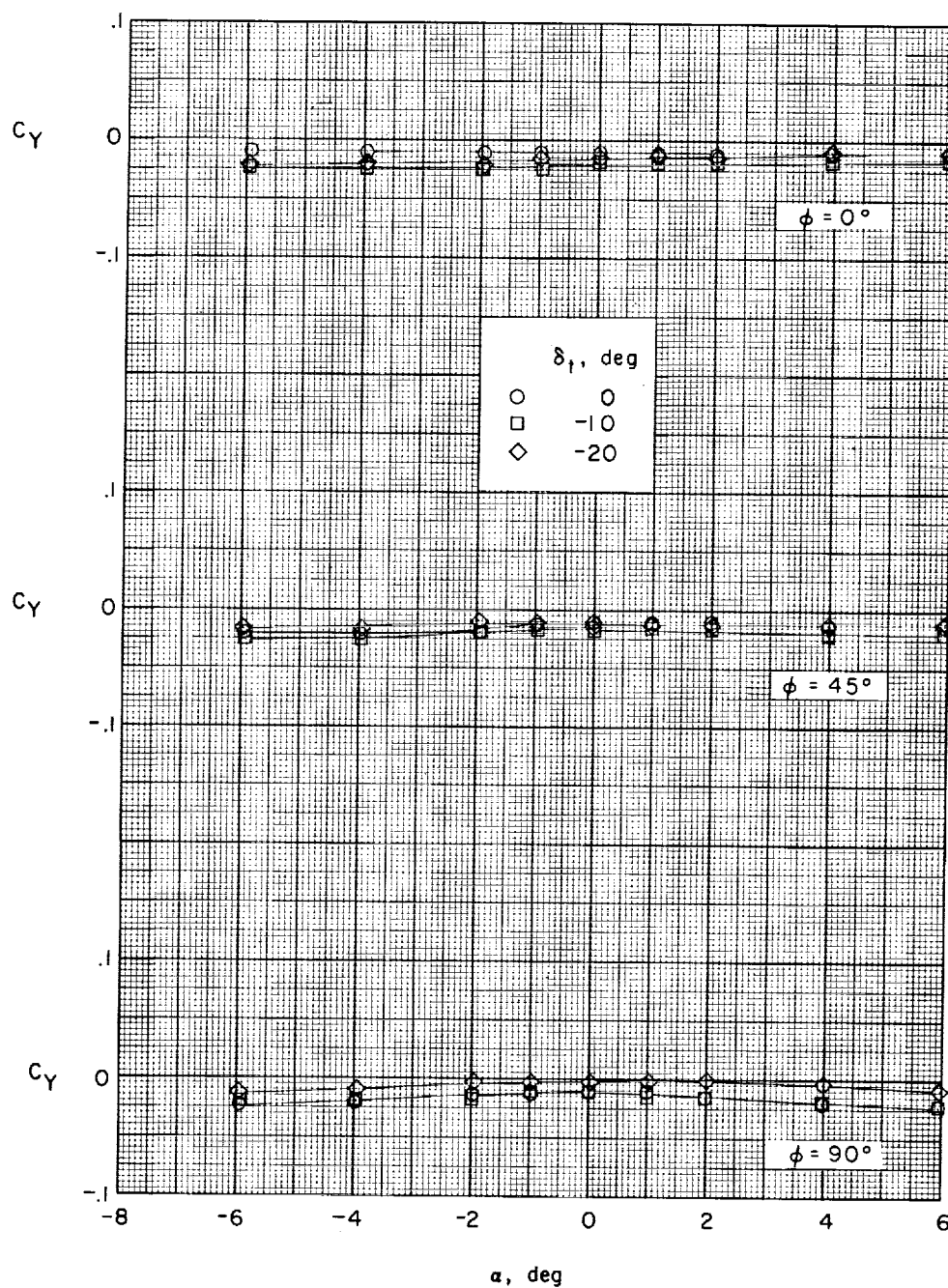
(a) Variation of C_Y with α.

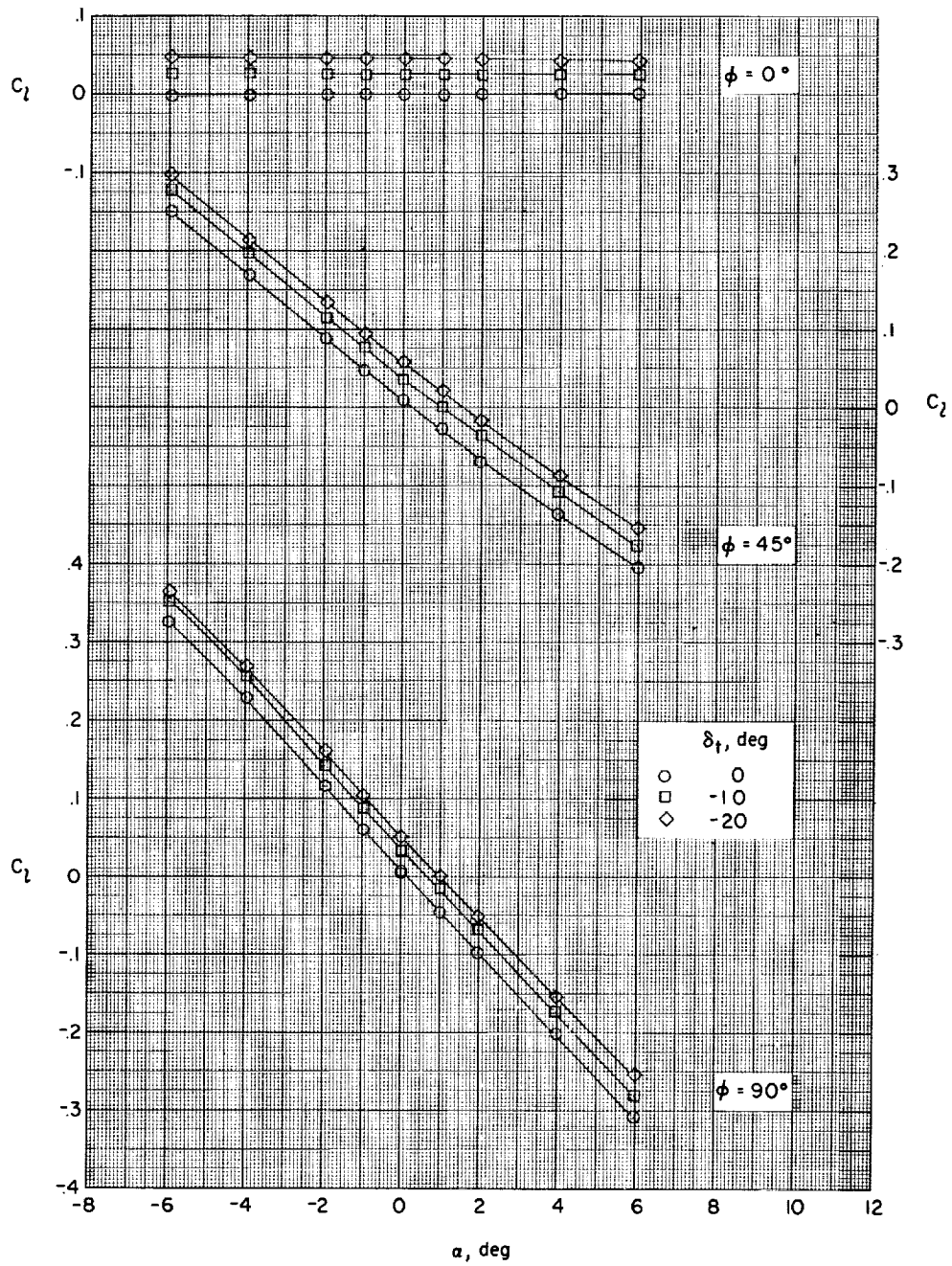Figure 6.- Effect of control deflection on side-force and shearing-moment coefficients for various roll angles.
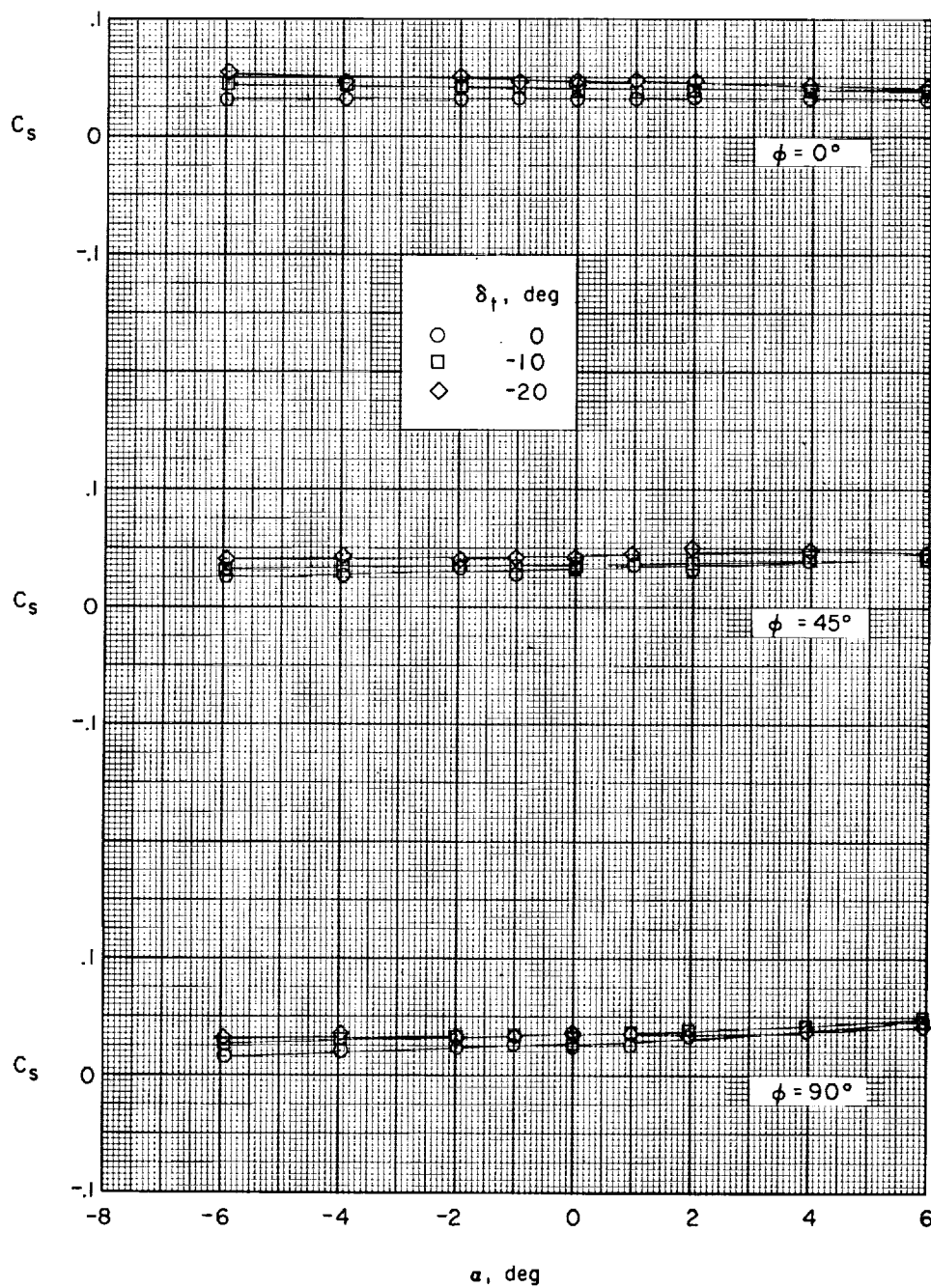
(b) Variation of C_S with α.

Figure 6.- Concluded.

(a) Variation of C_b with α.

Figure 7.- Effect of control deflection on root-bending-moment and rolling-moment coefficients for various roll angles.

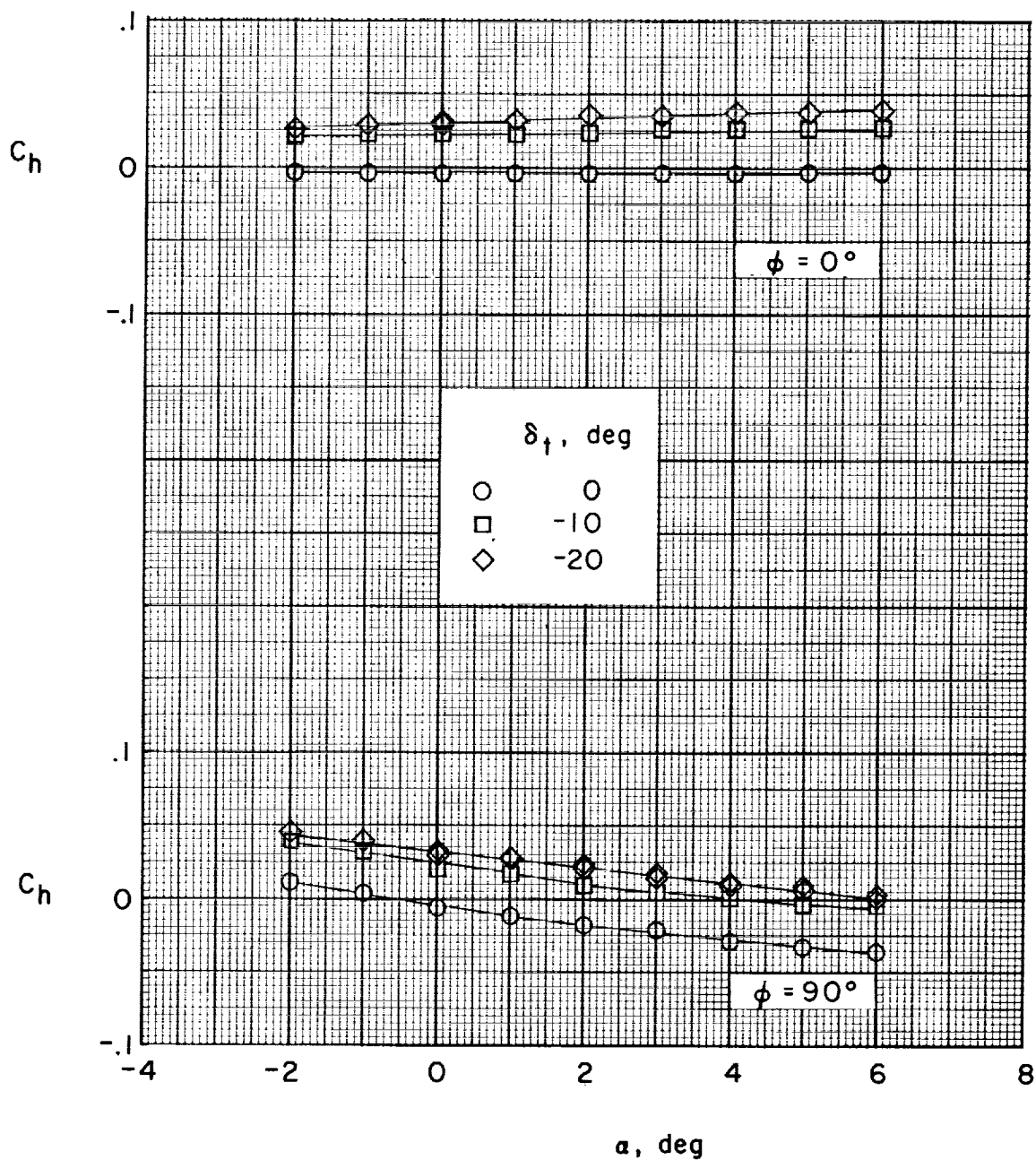(b) Variation of C_l with α.

Figure 7.- Concluded.

Figure 8.- Effect of control deflection on the hinge-moment coefficients for roll angles of 0° and 90°.